

# Size Control of Palladium Nanoparticles and Their Crystal Structures

T. Teranishi and M. Miyake\*

*School of Materials Science, Japan Advanced Institute of Science and Technology,  
1-1 Asahidai, Tatsunokuchi, Nomi-gun, Ishikawa 923-12, Japan*

*Received August 20, 1997. Revised Manuscript Received November 17, 1997*

The mean diameter of monodispersed Pd nanoparticles could be controlled from 17 to 30 Å in a one-step reaction by changing the amount of protective polymer, poly(*N*-vinyl-2-pyrrolidone) (PVP) and the kind and/or the concentration of alcohol in the solvent. Although increasing the amount of protective polymer made the size of Pd nanoparticles smaller, the particle size appeared to have a lower limit determined by the kind of alcohol. On the other hand, monodispersed Pd nanoparticles of smaller diameter were obtained in the order methanol > ethanol > 1-propanol, indicating that a faster reduction rate of  $[\text{PdCl}_4]^{2-}$  ions is an important factor to produce the smaller particles. The particle diameter showed a minimum at around 40 vol % of alcohol in solvent. Once the monodispersed Pd nanoparticles were obtained, the larger particles with a narrow size distribution could be easily synthesized by using the stepwise growth reaction. The Pd nanoparticles obtained here had fcc structures like that of bulk Pd, although the lattice constant increased with a decrease in the particle size.

## Introduction

Nanostructured transition metal nanoparticles are of great interest from both fundamental and practical viewpoints because of the quantum size effect, which is derived from the dramatic reduction of the number of free electrons.<sup>1,2</sup> Recently, Volokitin et al. have found that the quantum size effect strongly affected the thermodynamics of the metal nanoparticles.<sup>3</sup> Nanoparticles hold promise for use as advanced materials with new electronic, magnetic, optic, and thermal properties.<sup>4,5</sup> They have been also applied to catalysts<sup>6</sup> for hydrogenation of olefins and dienes,<sup>7,8</sup> hydration of acrylonitrile to acrylamide,<sup>9</sup> photogeneration of hydrogen from water,<sup>10,11</sup> and reduction of carbon dioxide,<sup>12,13</sup> the catalytic activity and selectivity being strongly affected by the particle size. To investigate the physical and chemical properties of metal nanoparticles, espe-

cially the size-dependent properties, precise control of the particle size is essentially required. Moreover, the precise control of particle size is also required for the organization of metal nanoparticles.<sup>14,15</sup>

It has been found from mass spectral studies that the binding energies of metal nanoparticles consisting fewer than ca. 1000 atoms vary periodically due to the quantum size effect.<sup>16,17</sup> This phenomenon was first found by Knight et al.<sup>18</sup> through experiments involving Na nanoparticles. This suggests the discontinuous existence of nanoparticles having certain stable structures. In the case of the noble metal nanoparticles, those with the atomic shell structures shown in Figure 1 are considered to be stable. Therefore, a synthetic technique is required to produce the nanoparticles with any sizes within a few angstroms in standard deviation.

The usual synthetic technique for making such nanoparticles involves chemical or electrochemical reduction of metal ions in the presence of a stabilizer such as linear polymers,<sup>8,9,19–23</sup> ligands,<sup>24–26</sup> surfactants,<sup>27–30</sup>

- (1) Halperin, W. P. *Rev. Mod. Phys.* **1986**, *58*, 533.
- (2) Schmid, G. *Clusters and Colloids*; VCH: Weinheim, 1994.
- (3) Volokitin, Y.; Sinzig, J.; de Jong, L. J.; Schmid, G.; Vargaftik, M. N.; Moiseev, I. I. *Nature* **1996**, *384*, 621.
- (4) Colvin, V. L.; Schlamp, M. C.; Alivisatos, A. P. *Nature* **1994**, *370*, 354.
- (5) Andres, R. P.; et al. *Chem. Eng. News* **1992**, Nov 18 (Nanostructured Materials Promise to Advance Range of Technologies).
- (6) Lewis, L. N. *Chem. Rev. (Washington, D.C.)* **1993**, *93*, 2693.
- (7) Hirai, H.; Toshima, N. *Tailored Metal Catalysts*; Iwasawa, Y., Ed.; D. Reidel: Dordrecht, 1986; pp 87–140.
- (8) Teranishi, T.; Nakata, K.; Miyake, M.; Toshima, N. *Chem. Lett.* **1996**, *277*; Teranishi, T.; Nakata, K.; Iwamoto, M.; Miyake, M.; Toshima, N. *React. Funct. Polym.*, in press.
- (9) Toshima, N.; Wang, Y. *Adv. Mater.* **1994**, *6*, 245.
- (10) Bard, A. J. *Science* **1980**, *207*, 139.
- (11) Toshima, N.; Kuriyama, M.; Yamada, Y.; Hirai, H. *Chem. Lett.* **1981**, 793.
- (12) Willner, I.; Maidan, R.; Mandler, D.; Dürr, H.; Dörr, G.; Zengerle, K. *J. Am. Chem. Soc.* **1987**, *109*, 6080.
- (13) Toshima, N.; Yamaji, Y.; Teranishi, T.; Yonezawa, T. *Z. Naturforsch.* **1995**, *50a*, 283.

- (14) Teranishi, T.; Hosoe, M.; Miyake, M. *Adv. Mater.* **1997**, *9*, 65.
- (15) Reetz, M. T.; Winter, M.; Tesche, B. *Chem. Commun.* **1997**, 147.
- (16) Sugano, S. *Microcluster Physics*; Springer-Verlag: Berlin, 1991.
- (17) Katakuse, I. *J. Mass Spectrom. Soc. Jpn.* **1994**, *42*, 67.
- (18) Knight, W. D.; Clemenger, K.; deHeer, W. A.; Saunders, W. A.; Chou, M. Y.; Cohen, M. *Phys. Rev. Lett.* **1984**, *52*, 2141.
- (19) Hirai, H.; Chawanya, H.; Toshima, N. *React. Polym.* **1985**, *3*, 127.
- (20) Toshima, N.; Harada, M.; Yonezawa, T.; Kushihashi, K.; Asakura, K. *J. Phys. Chem.* **1991**, *95*, 7448.
- (21) Henglein, A. *J. Phys. Chem.* **1993**, *97*, 5457.
- (22) Bradley, J. S.; Millar, J. M.; Hill, E. W.; Behal, S.; Chaudret, B.; Duteil, A. *Faraday Discuss.* **1991**, *92*, 255.
- (23) Hirai, H.; *J. Macromol. Sci.-Chem.* **1979**, *A13*, 633. Bradley, J. S.; Hill, E. W.; Behal, S.; Klein, C. *Chem. Mater.* **1992**, *4*, 1234.
- (24) Schmid, G. *Chem. Rev. (Washington, D.C.)* **1992**, *92*, 1709.
- (25) Poulin, J. C.; Kagan, H. B.; Vargaftik, M. N.; Stolarov, I. P.; Moiseev, I. I. *J. Mol. Catal.* **1995**, *95*, 109.

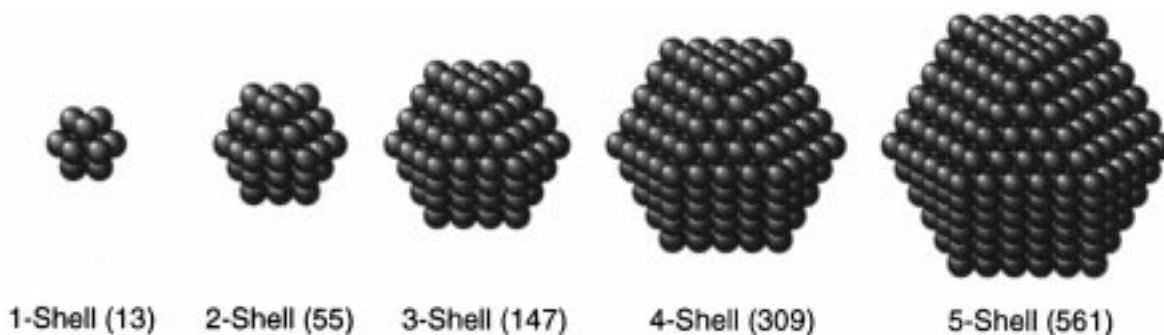


**Figure 1.** Shell structures of noble metal nanoparticles.

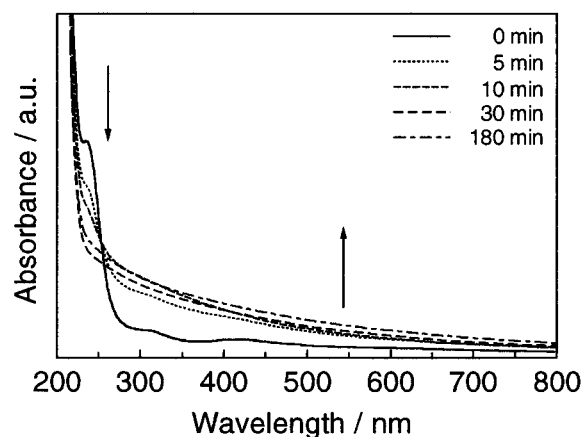


**Figure 2.** UV-vis spectral change during the formation of PVP-Pd nanoparticles (PVP/Pd = 10, [ethanol] = 20 vol %).

tetraalkylammonium salts,<sup>31–35</sup> or heterogeneous supports,<sup>36–39</sup> which prevent the nanoparticles from aggregating and allow one to isolate the nanoparticles. To control the particle size, the stabilizer, reducing agent, solvent, and so on have been varied as parameters. Control of particle size by using the ligands has been extensively studied,<sup>24</sup> many shell-structured nanoparticles being synthesized, such as 2-shell Au,<sup>40</sup> 4-shell Pt,<sup>41</sup> and 5, 7, and 8-shell Pd<sup>42–44</sup> nanoparticles. On the other hand, few reports on the size control of metal nanoparticles in the presence of linear polymers have appeared.<sup>23</sup> When a linear polymer is used as a protective agent, modification of the functional groups can

offer a specific reaction field around the metal nanoparticles that promotes the catalytic activity of the nanoparticles and may change the electronic structures of the metal nanoparticles.<sup>8</sup> Recently, Ahmadi et al. succeeded in controlling the shape of Pt nanoparticles by using sodium polyacrylate as a capping polymer.<sup>45</sup> We have controlled the size of Pt nanoparticles by using poly(*N*-vinyl-2-pyrrolidone) and succeeded in their two-dimensional organization.<sup>14</sup> Thus, linear polymers have great potential as protective agents for nanoparticles.

In the present study, we used poly(*N*-vinyl-2-pyrrolidone) as a stabilizer for Pd nanoparticles. The experimental conditions, such as the amount of the protective polymer and the kind and/or the concentration of reducing agent, are systematically changed to control the particle size of Pd nanoparticles. Then, the stepwise growth of Pd nanoparticles was investigated to obtain monodispersed Pd nanoparticles having >30 Å in diameter. The change in the lattice constant with decreasing size of the Pd nanoparticles was also observed.

## Experimental Section

**Materials.** Palladium chloride (Kanto Chemicals) was used as purchased. Poly(*N*-vinyl-2-pyrrolidone) (PVP, average molecular weight 40 000, Kanto Chemicals) was used as a standard protective polymer for the Pd nanoparticles. Methanol, ethanol, 1-propanol, and diethyl ether were guaranteed grade and used without further purification.

**Synthetic Procedure of PVP-Protected Pd Nanoparticles.** H<sub>2</sub>PdCl<sub>4</sub> aqueous solution (2.0 mM) was prepared by mixing 106.4 mg of PdCl<sub>2</sub> (0.6 mmol), 6.0 mL of 0.2 M HCl, and 294 mL of distilled water. A mixture of 15 mL of 2.0 mM H<sub>2</sub>PdCl<sub>4</sub> aqueous solution (30 μmol of Pd), *x* mL of water, *y* mL of alcohol (*x* + *y* = 35 mL), and the designated amount of PVP was refluxed in a 100 mL flask for 3 h under air to synthesize the PVP-protected Pd nanoparticles (abbreviated as PVP-Pd). The amount of PVP was also altered from 0.333 to 133 mg (3.0 to 1200 μmol as a monomeric unit) in order to control the size and size distribution of Pd nanoparticles. The concentration of alcohol in the solvent was changed from 10 to 70 vol % in order to investigate the dependence of the size and size distribution of Pd nanoparticles on the reduction rate of [PdCl<sub>4</sub>]<sup>2-</sup>.

(26) Amiens, C.; de Caro, D.; Chaudret, B.; Bradley, J. S.; Mazel, R.; Roucau, C. *J. Am. Chem. Soc.* **1993**, *115*, 11638.

(27) Toshima, N.; Takahashi, T. *Bull. Chem. Soc. Jpn.* **1992**, *65*, 400.

(28) Yonezawa, T.; Tominaga, T.; Toshima, N. *Langmuir* **1995**, *11*, 4601.

(29) Esumi, K.; Matsuhisa, K.; Torigoe, K. *Langmuir* **1995**, *11*, 3285.

(30) Leff, D. V.; Ohara, P. C.; Heath, J. R.; Gelbart, W. M. *J. Phys. Chem.* **1995**, *99*, 7036.

(31) Bönemann, H.; Brijoux, W.; Brinkmann, R.; Dinjus, E.; Jousen, T.; Korall, B. *Angew. Chem., Int. Ed. Engl.* **1991**, *30*, 1312.

(32) Bönemann, H.; Brijoux, W.; Brinkmann, R.; Fretzen, R.; Jousen, T.; Köppler, R.; Korall, B.; Neiteler, P.; Richter, J. *J. Mol. Catal.* **1994**, *86*, 129.

(33) Reetz, M. T.; Helbig, W. *J. Am. Chem. Soc.* **1994**, *116*, 7401.

(34) Reetz, M. T.; Helbig, W.; Quaiser, S. A.; Stimming, U.; Breuer, N.; Vogel, R. *Science* **1995**, *267*, 367.

(35) Reetz, M. T.; Quaiser, S. A. *Angew. Chem., Int. Ed. Engl.* **1995**, *34*, 2240.

(36) Toshima, N.; Teranishi, T.; Asanuma, H.; Saito, Y. *J. Phys. Chem.* **1992**, *96*, 3796.

(37) Teranishi, T.; Toshima, N. *J. Chem. Soc., Dalton Trans.* **1994**, 2967.

(38) Teranishi, T.; Toshima, N. *J. Chem. Soc., Dalton Trans.* **1995**, 979.

(39) Tauster, S. J. *Acc. Chem. Res.* **1987**, *20*, 389.

(40) Schmid, G.; Giebel, U.; Huster, W.; Schwenk, A. *Inorg. Chim. Acta* **1984**, *85*, 97.

(41) Schmid, G.; Morun, B.; Malm, J.-O. *Angew. Chem., Int. Ed. Engl.* **1989**, *28*, 778.

(42) Vargaftik, N. M.; Moiseev, I. I.; Kochubey, D. I.; Zamaraev, K. I. *Faraday Discuss. Chem. Soc.* **1991**, *92*, 13.

(43) Schmid, G. *Polyhedron* **1988**, *7*, 2321.

(44) Schmid, G.; Harms, M.; Malm, J.-O.; Bovin, J.-O.; van Ruitenbeck, J.; Zandbergen, H. W.; Fu, W. T. *J. Am. Chem. Soc.* **1993**, *115*, 2046.

(45) Ahmadi, T. S.; Wang, Z. L.; Green, T. C.; Henglein, A.; El-Sayed, M. A. *Science* **1996**, *272*, 1924.

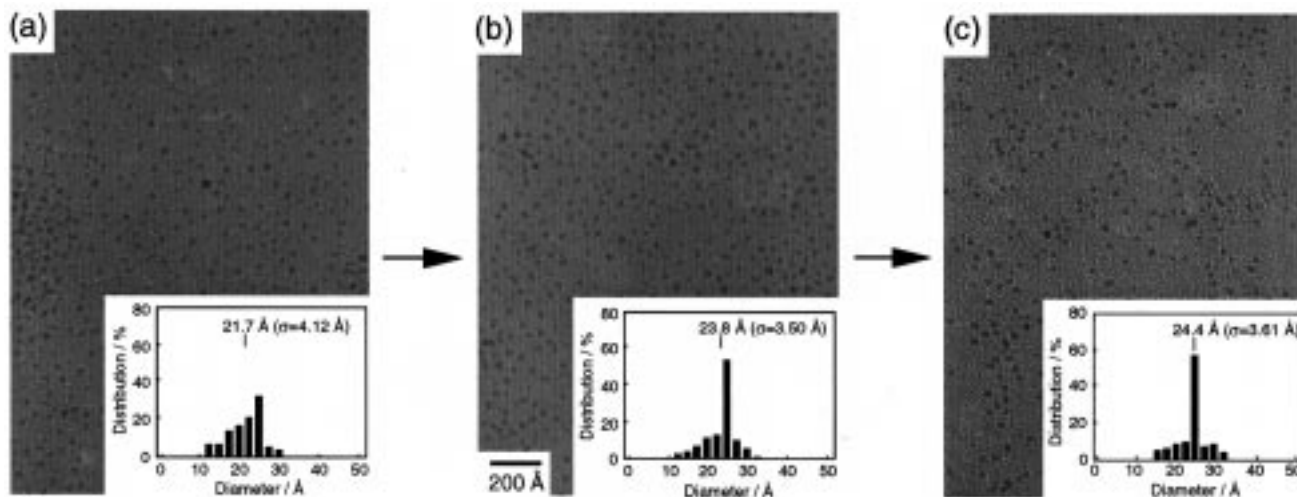


**Figure 3.** Change in size of PVP–Pd nanoparticles with increasing refluxing time. The refluxing time are (a) 15 min, (b) 30 min, (c) 180 min (PVP/Pd = 10, [ethanol] = 20 vol %).

**Measurements.** The colloidal dispersions of the PVP–Pd nanoparticles have a dark brown color and are stable for months at room temperature. The disappearance of  $[\text{PdCl}_4]^{2-}$  ions and the formation of Pd nanoparticles were confirmed by UV–vis spectra with a Shimadzu UV-2200 UV–vis recording spectrophotometer. The PVP–Pd nanoparticles were characterized by transmission electron microscopy (TEM) and selected area electron diffraction (ED) at 125 kV on a Hitachi H-7100 electron microscope. Samples for TEM and ED were prepared by placing a drop of the colloidal dispersion of PVP–Pd nanoparticles onto a carbon-coated copper grid, followed by naturally evaporating the solvent. The mean diameter and standard deviation were calculated by counting 200 particles with a loupe from the TEM image of 400 000 magnifications. The crystallinity of the PVP–Pd nanoparticles was confirmed by high-resolution TEM (HRTEM) at 300 kV on a Hitachi H-9000NAR. The crystal structure of the PVP–Pd nanoparticles was also investigated by X-ray powder diffraction (XRD) on a Rigaku Rint 2000 X-ray diffractometer with  $\text{Cu K}\alpha$  radiation. Samples for XRD measurement were prepared by precipitating the PVP–Pd nanoparticles with a large amount of diethyl ether, followed by filtering and drying under vacuum at 90 °C, and then crushing them with a mortar. X-ray photoelectron spectroscopy (XPS) was employed to confirm whether the surface Pd atoms of the PVP–Pd nanoparticles synthesized in air were oxidized or not. The Pd 3d peaks of PVP–Pd nanoparticles synthesized in ethanol/water (1/4, v/v) both under air and  $\text{N}_2$  were measured on a Ulvac Phi 5600ci with monochromated Al X-ray at 350 W.

## Results and Discussion

**Formation of Pd Nanoparticles.** The formation process of PVP-protected Pd nanoparticles (PVP/Pd = 10, mol/mol) synthesized in ethanol/water (1/4, v/v) is presented as a representative example. The solution before reflux is pale yellow and shows a peak at 235 nm in its UV–vis spectrum due to the ligand-to-metal charge-transfer transition of the  $[\text{PdCl}_4]^{2-}$  ions, as shown in Figure 2. As the refluxing time increases, the peak at 235 nm decreases and disappears within 30 min, indicating that the  $[\text{PdCl}_4]^{2-}$  ions are completely reduced in 30 min. The color of the solution turns from pale yellow into dark brown and the absorption from the ultraviolet to the visible region increases, suggesting that the band structure of the Pd nanoparticles is formed. Figure 3 presents the change in particle size of the PVP–Pd nanoparticles with increasing refluxing time. The size of the Pd nanoparticles formed in 30 min

is almost the same as that formed in 180 min, in good agreement with the UV–vis results.

Since the XPS measurements of the PVP–Pd synthesized both under air and under nitrogen indicated no difference in the Pd 3d<sub>5/2</sub> peak position at 336.1 eV and shape, the PVP–Pd synthesized under air was concluded not to be oxidized. Storage of PVP–Pd under oxygen for a few weeks, however, gave a new peak at a higher binding energy of 337.4 eV, which corresponds to the oxidized Pd.

**Size Control of Pd Nanoparticles by Variation of the Amount of PVP.** The protective polymer, PVP, apparently stabilizes the Pd nanoparticles by preventing them from aggregating. Hirai et al.<sup>15</sup> showed that the carbonyl groups of PVP partly coordinate to the surface Pd atoms of the Pd nanoparticles. Such coordination was also confirmed by our FT-IR measurement. Part of the main chain of PVP is also expected to be adsorbed on the surface Pd atoms by hydrophobic interaction. Accordingly, the amount of PVP added to the solution is expected to affect the growth process for the Pd nanoparticles. Therefore, the change in size of the Pd nanoparticles was investigated by varying the amount of PVP. Figure 4 shows the mean diameters and standard deviations of PVP–Pd synthesized at various molar ratios of PVP/Pd in ethanol/water under reflux for 3 h. As might be anticipated, at PVP/Pd = 0.1, PVP–Pd nanoparticles of mean diameter larger than 30 Å with quite a wide distribution are obtained at any concentration of alcohol. At PVP/Pd = 1.0, we obtained PVP–Pd nanoparticles smaller than 30 Å in mean diameter with 20–50 vol % of ethanol. The PVP–Pd nanoparticles synthesized at PVP/Pd = 10 and 40 have mean diameters from 22 to 25 Å and 17 to 21 Å with a narrow distribution ( $\sigma < 5$  Å) with 20–40 vol % of ethanol, respectively. Palladium nanoparticles having a mean diameter of 24.4 Å ( $\sigma = 3.61$  Å) are obtained at 20 vol % of ethanol at PVP/Pd = 10, which corresponds to a 5-shell structure consisting of the magic number of 561 atoms. It appears that the particle with the smallest size is produced at 20–40 vol % of alcohol when excess amount of PVP to Pd is added.

**Size Control of Pd Nanoparticles by Kind and Concentration of Alcohol.** As shown in Figure 4, the

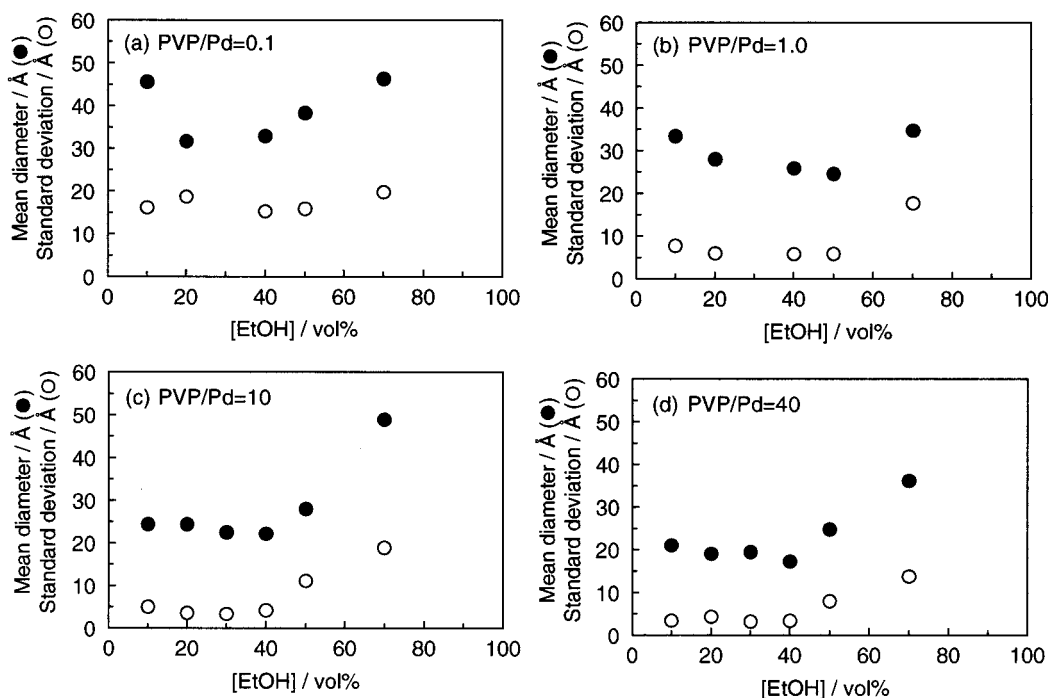


**Figure 4.** Mean diameters and standard deviations of PVP–Pd nanoparticles synthesized at various PVP/Pd ratios. PVP/Pd = (a) 0.1, (b) 1.0, (c) 10, (d) 40.

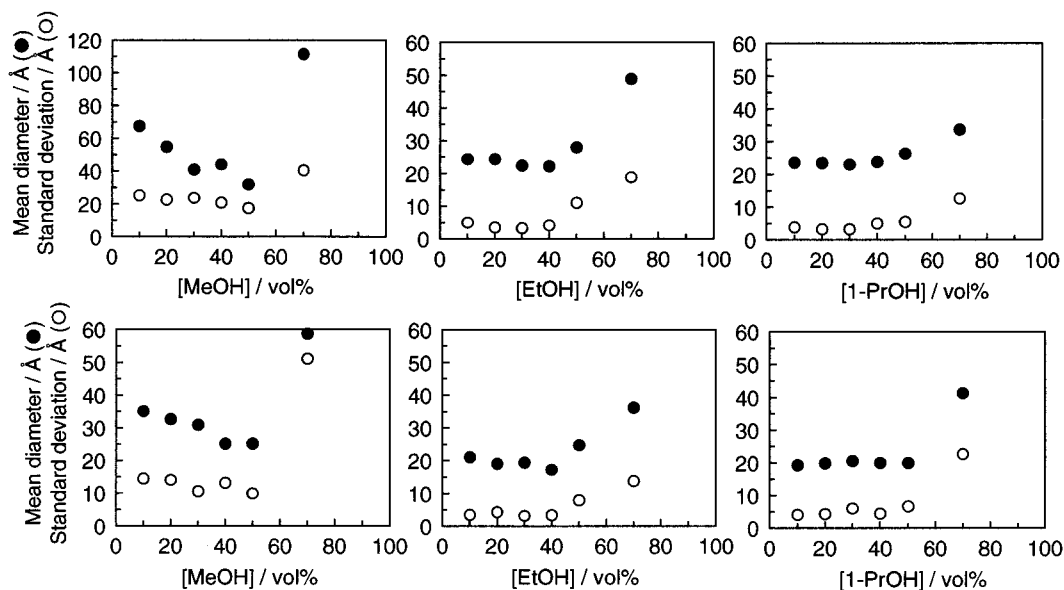


**Figure 5.** Mean diameters and standard deviations of PVP–Pd nanoparticles synthesized at various alcohol concentration. PVP/Pd = 10 (upper), 40 (lower).

mean diameter of the PVP–Pd particles shows a minimum at 20–50 vol % of ethanol, implying that the size of the PVP–Pd nanoparticles is greatly influenced by the kind and concentration of alcohol used as a reducing agent. An appropriate choice of the kind and the concentration of the reducing agent is important in controlling the particle size, because the reduction rate of  $[\text{PdCl}_4]^{2-}$  to  $\text{Pd}^0$  are greatly affected by the kind and the concentration of the reducing agent. Figure 5 shows the mean diameters and standard deviations of the PVP–Pd nanoparticles, which were systematically synthesized by changing the kind and concentration of alcohol at the PVP/Pd ratios of 10/1 and 40/1 under reflux for 3 h. Methanol, ethanol, and 1-propanol were employed at concentrations of 10–70 vol % in water.

From the viewpoint of the kind of alcohol, both the particle size and the standard deviation become smaller in the order of methanol > ethanol > 1-propanol at any alcohol/water ratio; this tendency corresponds to their increasing boiling points. Furthermore, from the viewpoint of the hydrogenation enthalpies of the corresponding aldehydes, methanol is unfavorable to be oxidized in comparison with ethanol and 1-propanol. Thus, it is suggested that the reduction of  $[\text{PdCl}_4]^{2-}$  by the alcohol with higher boiling point produces more Pd nuclei in a shorter period and suppresses the growth of Pd nanoparticles, that is, a faster reduction rate of  $[\text{PdCl}_4]^{2-}$  is needed to generate the smaller Pd nanoparticles with narrower distribution.

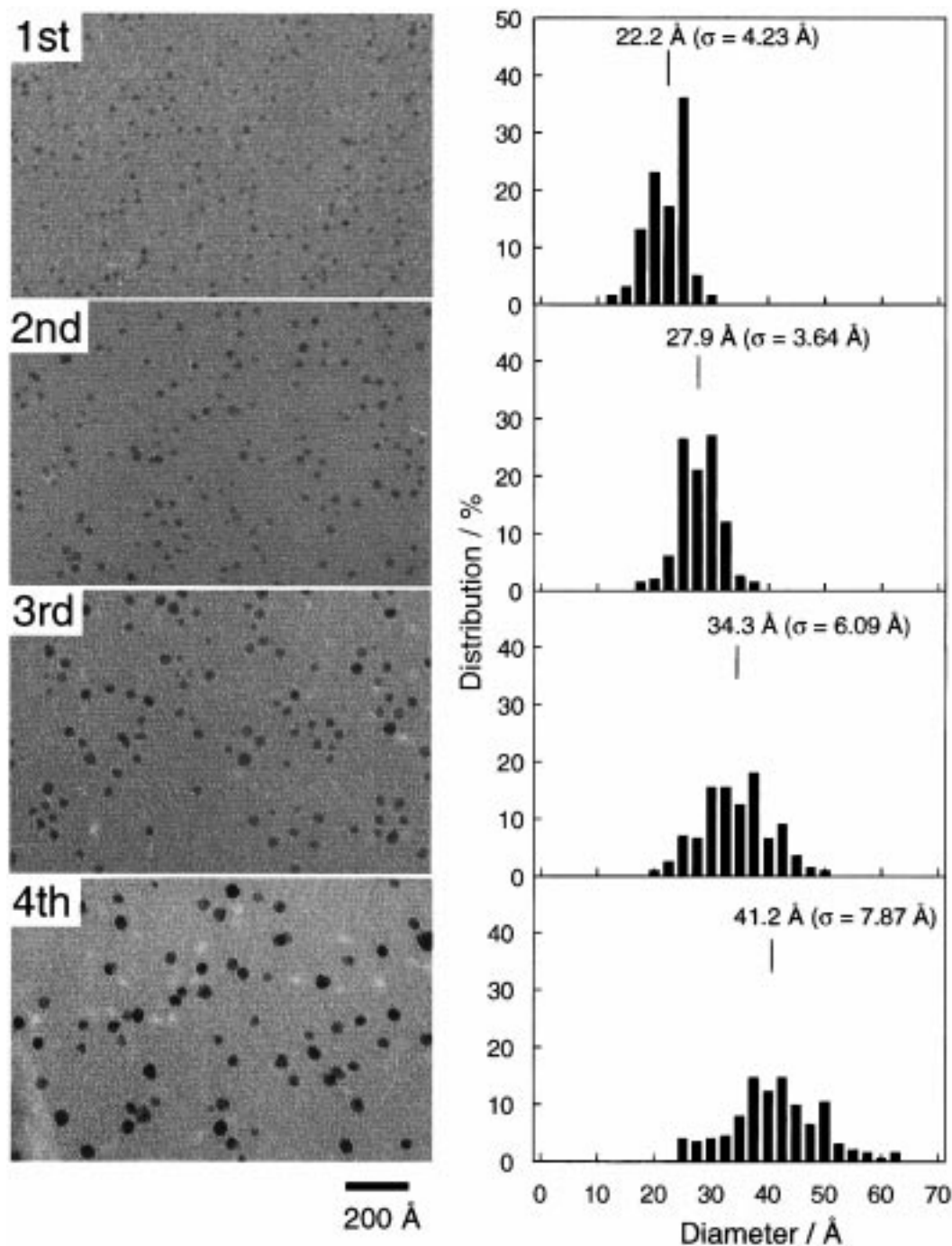


**Figure 6.** TEM photographs of PVP-Pd nanoparticles synthesized by the stepwise growth and size distributions estimated from the photographs (PVP/Pd = 10, [ethanol] = 40 vol %).

In general, an increase in the concentration of the reducing agent increases the reduction rate of metal ions, leading to smaller metal nanoparticles. However, the mean diameters and standard deviations of the PVP-Pd nanoparticles synthesized by using any alcohols reach a minimum at around 40 vol % of alcohol. The PVP dissolves in both alcohol and water to disperse completely in alcohol/water mixed solution, although  $\text{H}_2\text{PdCl}_4$  does not dissolve in alcohol. Therefore,  $\text{H}_2\text{PdCl}_4$  does not homogeneously disperse in solution at the higher concentrations of alcohol, resulting in a larger size and wider distribution of PVP-Pd nanoparticles. At lower concentrations of alcohol, both the PVP and  $\text{H}_2\text{PdCl}_4$  homogeneously disperse in solution, but the reduction rate of  $[\text{PdCl}_4]^{2-}$  decreases, especially in

the case of methanol, resulting in the formation of larger particles. Consequently, a minimum in the particle sizes appeared as shown in Figures 4 and 5. This result leads us to the suggestion that using the alcohol-soluble metal precursor makes the particle size smaller at a higher concentration of alcohol in the solvent. In fact, in the case of the PVP-protected Pt nanoparticles, the size of the Pt nanoparticles became smaller at a higher alcohol concentration in the solvent by using  $\text{H}_2\text{PtCl}_6$  as an alcohol-soluble precursor.<sup>14,46</sup>

At 20–40 vol % of ethanol, 25 Å Pd nanoparticles with a 5-shell structure and 20 Å Pd nanoparticles with a 4-shell structure are obtained as the major particles at

PVP/Pd = 10 and 40, respectively. Especially, 5-shell Pd nanoparticles were selectively synthesized in an ethanol/water (1/4, v/v) mixed solvent at the molar ratio of PVP/Pd = 10. We have already pointed out through ESR measurement of Pd nanoparticles that the 25 Å Pd nanoparticles with 5-shell structure have the closed-electron shell structure, that is, they are in a spin-singlet state.<sup>47</sup>

**Stepwise Growth of Pd Nanoparticles.** A one-step synthesis is adequate to obtain the Pd nanoparticles of 10–30 Å, while it is quite difficult to synthesize the Pd nanoparticles larger than 30 Å in a one-step reaction. So, the monodispersed PVP–Pd nanoparticles synthesized in a one-step reaction were used for stepwise growth to obtain nanoparticles larger than 30 Å in mean diameter without changing the size distribution. The PVP–Pd nanoparticles synthesized in ethanol/water (2/3, v/v) at PVP/Pd = 10 have a mean diameter of 22.2 Å with a narrow size distribution ( $\sigma = 4.23$  Å), so they were employed as the starting particles for stepwise growth. A second growth of PVP–Pd nanoparticles was carried out by mixing 25 mL of 0.6 mM PVP–Pd dispersion with 25 mL of a 0.6 mM H<sub>2</sub>-PdCl<sub>4</sub> in ethanol/water (2/3, v/v) solution, followed by refluxing the mixture for 3 h. A third and fourth growth were conducted in the same way. The TEM photographs and size distributions of PVP–Pd obtained at each growth step are shown in Figure 6. The nanoparticles are clearly growing with increasing growth steps, indicating that the nanoparticles in the solution serve as nuclei for larger ones. The diameter of nanoparticles to be obtained,  $d$ , can be calculated by the eq 1:<sup>24</sup>

$$d = d_0 \sqrt[3]{\frac{n_i + n_m}{n_m}} \quad (1)$$

where  $d_0$  = particle diameter in the starting solution and  $n_i$ ,  $n_m$  = quantity of the ionic and metallic Pd, respectively. In our case,  $n_i = n_m$ , so formula 1 leads to eq 2:

$$d = \sqrt[3]{2} d_0 \quad (2)$$

The mean diameters of PVP–Pd estimated by the TEM photographs are 22.2, 27.9, 34.3, and 41.2 Å, while those calculated from eq 2 are 22.2, 28.0, 35.2, and 44.4 Å. The experimental results show a slightly smaller diameter than the calculated ones, and a gradual expansion of the size distribution. The first particles are distributed from 12.5 to 30.0 Å. Assuming that each particle grows according to eq 2, the second particles are predicted to have a size distribution from 15.7 to 37.8 Å. The third and fourth particles should have size distributions from 19.8 to 47.6 Å and 24.8 to 60.0 Å, respectively. Those results are in good agreement with the experimental ones, indicating that the size distribution of the starting particles greatly influence that of the stepwise-synthesized particles. Therefore, the application of separation procedures, such as HPLC<sup>21</sup> or fractional precipitation,<sup>48</sup> to Pd nanoparticles obtained

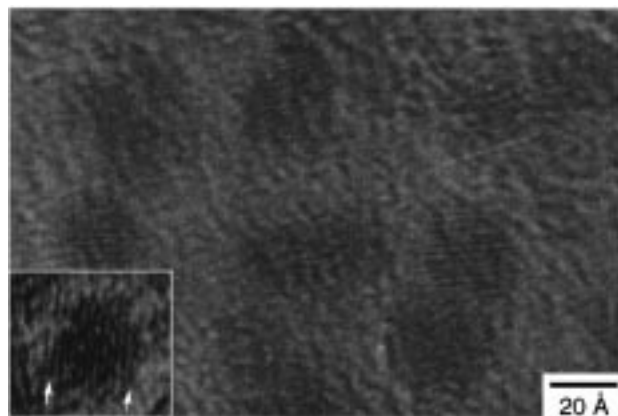


**Figure 7.** The 300 kV HRTEM image of PVP–Pd nanoparticles (PVP/Pd = 10, [ethanol] = 20 vol %).

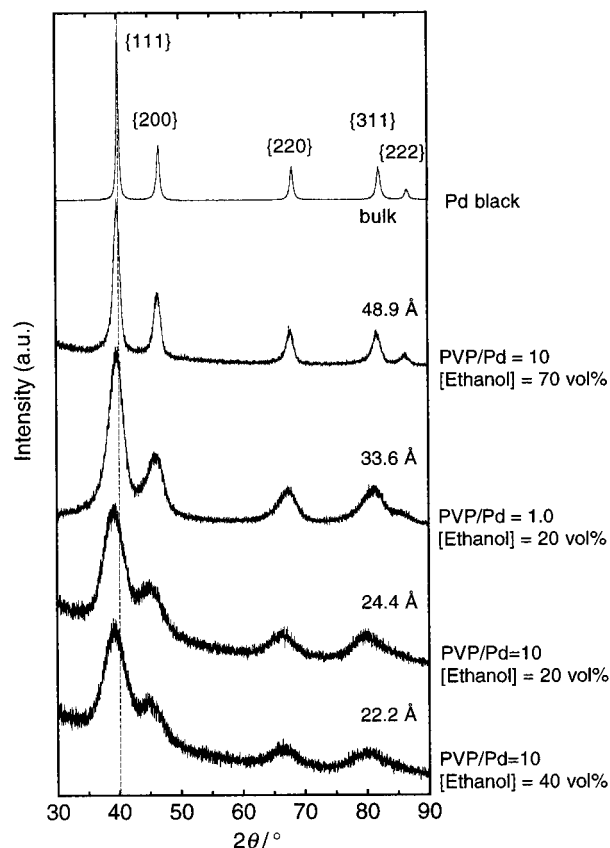


**Figure 8.** XRD patterns of PVP–Pd nanoparticles of various diameters.

by a one-step reaction may be effective to synthesize larger particles with a narrow size distribution.

**Crystal Structure of the Pd Nanoparticles.** The crystal structures of the PVP–Pd nanoparticles were investigated by HRTEM, XRD, and ED. Figure 7 presents a HRTEM image of PVP–Pd nanoparticles synthesized in ethanol/water (1/4, v/v) at PVP/Pd = 10. All the Pd nanoparticles show lattice images, so that they are single crystallites. Since 11 {111} layers are observed, these nanoparticles are concluded to have a 5-shell structure. The XRD patterns of Pd black and PVP–Pd nanoparticles with mean diameters of 22.2, 24.4, 33.6, and 48.9 Å are shown in Figure 8. Several peaks are observed in each XRD pattern at around 40°, 46°, 68°, 82°, and 86°. These peaks correspond to the {111}, {200}, {220}, {311}, and {222} planes of a fcc

(47) Teranishi, T.; Hori, H.; Miyake, M. *J. Phys. Chem. B* **1997**, *101*, 5774.

(48) Taleb, A.; Petit, C.; Pileni, M. P. *Chem. Mater.* **1997**, *9*, 950.

**Table 1. Diffraction Angle, Interplanar Spacing of {111} Plane, and Lattice Constant of PVP–Pd Nanoparticles of Various Diameters**

synthetic condition	mean diam/Å	$2\theta$ of {111}/deg	$d^a/\text{Å}$	$a^b/\text{Å}$
JCPDS database		40.113	2.2460	3.8902
Pd black		40.080	2.2478	3.8933
PVP/Pd = 10, [ethanol] = 70 vol %	48.9	39.860	2.2597	3.9139
PVP/Pd = 1.0, [ethanol] = 20 vol %	33.6	39.660	2.2707	3.9330
PVP/Pd = 10, [ethanol] = 20 vol %	24.4	39.220	2.2951	3.9752
PVP/Pd = 10, [ethanol] = 40 vol %	22.2	39.260	2.2929	3.9714

<sup>a</sup> {111} interplanar spacing. <sup>b</sup> Lattice constant.

lattice, respectively, indicating that the PVP–Pd nanoparticles synthesized in the present study have the fcc structure. Selected area ED showed four Debye–Scherrer rings assigned to {111}, {200}, {220}, and {311} planes, which supported the XRD results.

In Figure 8, the diffraction angles are found to be shifted toward lower values with a decrease in the particle size. This means that the Pd–Pd interatomic distance expands with a decrease in the particle size in contrast with the PVP–Pt nanoparticles.<sup>46</sup> Table 1 summarizes the diffraction angle, the interplanar spacing of {111} plane, and the lattice constant. It is known that the lattice constant of small metal nanoparticles decrease with their size.<sup>49–53</sup> The lattice contraction can be explained by the theoretical treatment developed by

Vermaak et al.<sup>50</sup> According to their work, the observed lattice contraction can be interpreted in terms of a surface stress. Contrary to the other metals, a lattice constant gradually increases from Pd black to PVP–Pd of 24.4 Å, although both the PVP–Pd of 24.4 and 22.2 Å seems to have almost the same values because of small difference in their sizes. The dilation of the lattice constant has been observed not only by us but also by other scientists.<sup>54–56</sup> The dilation of the lattice constant is considered to be due to a structural change<sup>54</sup> or incorporation of oxygen,<sup>57</sup> carbon,<sup>58</sup> or hydrogen<sup>59</sup> into the Pd lattice. On the contrary, a report that the lattice constant of Pd nanoparticles decreases with their size, similar to that of the other metals has also appeared.<sup>60</sup> In our system, the reason for the dilation of the lattice constant is unresolved, but this is an interesting phenomena that has been observed only in Pd nanoparticles at present.

**Acknowledgment.** The present work was supported by a Grant-in-Aid for Scientific Research in Priority Areas of “New Polymers and Their Nano-organized Systems” (No. 08246224) and for Scientific Research on Encouragement Research (A) (No. 09740519) from the Ministry of Education, Science, Sports and Culture, Japan.

CM9705808

- (49) Berry, C. R. *Phys. Rev.* **1952**, *88*, 596.  
 (50) Vermaak, J. S.; Mays, C. W.; Kuhlmann-Wilsdorf, D. *Surf. Sci.* **1968**, *12*, 128.  
 (51) Mays, C. W.; Vermaak, J. S.; Kuhlmann-Wilsdorf, D. *Surf. Sci.* **1968**, *12*, 134.  
 (52) Wassermann, H. J.; Vermaak, J. S. *Surf. Sci.* **1972**, *32*, 168.  
 (53) Montano, P. A.; Zhao, J.; Ramanathan, M.; Shenoy, G. K.; Schulze, W.; Urban, J. *Chem. Phys. Lett.* **1989**, *164*, 126.

- (54) Heinemann, K.; Poppa, H. *Surf. Sci.* **1985**, *156*, 265.  
 (55) Giorgio, S.; Henry, C. R.; Chapon, C.; Penisson, J. M. *J. Cryst. Growth* **1990**, *100*, 254.  
 (56) Goyhenex, C.; Henry, C. R.; Urban, J. *Philos. Mag. A* **1994**, *69*, 1073.  
 (57) Jacobs, J. W.; Schryvers, D. S. *J. Catal.* **1987**, *103*, 436.  
 (58) Lamber, R.; Jaeger, N.; Schulz-Ekloff, G. *Surf. Sci.* **1990**, *227*, 15.  
 (59) Kuhrt, C.; Anton, R. *Thin Solid Films* **1991**, *198*, 301.  
 (60) Lamber, R.; Wetjen, S.; Jaeger, N. I. *Phys. Rev. B* **1995**, *51*, 10968.